Available online at www.sciencedirect.com

ScienceDirect

Procedia CIRP 46 (2016) 201 – 204

www.elsevier.com/locate/procedia

7th HPC 2016 – CIRP Conference on High Performance Cutting

FEM based modeling of cylindrical grinding process incorporating wheel topography measurement

Ali Zahedi[a,*], Bahman Azarhoushang[a]

[a]*Institute of Precisioin Machining (KSF), Furtwangen University of Applied Sciences, Jakob-Kienzle-Strasse 17, 78056 Villingen-Schwenningen, Germany*
[b]*Second affiliation, Address, City and Postcode, Country*

* Corresponding author. Tel.: +49-7720-9979811; fax: +49-7720-955779. *E-mail address:* ali.zahedi@hs-furtwangen.de

Abstract

In this research, the interaction of cBN cutting grains with a 100Cr6 bearing steel workpiece is simulated using Finite Element Method (FEM). Grinding conditions are associated with high temperatures and strain-rates. Therefore, a constitutive material model is used which accounts for the coupled temperature and strain-rate effects on the flow stress. Furthermore, as one of the main challenges in grinding analysis, the topography of the grinding wheel is modelled according to its actual confocal images. The parameters of a probability density function are extracted from the confocal microscopy data and the distribution of the cutting grains are accordingly defined. Through a transient kinematical approach, the single-grain model is extended to the aggregate action of cutting grains on the wheel surface in cylindrical grinding process of a 100Cr6 bearing steel. The simulation results are validated with experimental data.

Peer-review under responsibility of the International Scientific Committee of 7th HPC 2016 in the person of the Conference Chair Prof. Matthias Putz

Keywords: single-grain scratch; finite element method; cylindrical grinding; cBN grinding wheel; wheel topography; Gamma distribution

1. Introduction

In recent years, the grinding research has been focused on the fundamental understanding of material removal mechanisms in the micro-scale (single grain-workpiece interaction) [1]. Thanks to the advances in numerical techniques and computational processing units, Finite Element Method (FEM) has been extensively used to model various aspects of the grinding process, especially the cutting behavior of the individual abrasive grains in micro-scale [2]. Though, the micro-scale numerical modeling approaches should be able to describe the plastic behavior of the workpiece material at high temperatures and strain-rates associated with grinding [3]. Many material models have been used for the numerical simulation of metal cutting processes, which treated the workpiece as an elastic [4,5], elastoplastic [6] or a thermoplastic [7,8] medium. The Johnson-cook model is a common model for machining at high temperatures, strains and strain-rates [9]. Though, in the case of grinding where high temperatures and strain-rates are common, the constitutive laws should consider the coupled effects of temperature and strain-rate in addition to their individual contribution to the material behavior [10,11]. Accordingly, the coupled effects of work-hardening and thermal softening can be addressed in the considered range of cutting parameters.

The random shape and orientation of the cutting grains along with the probabilistic nature of the grinding wheel surface topography are further limitations in the numerical modeling of grinding process. The distribution and shape of the cutting grains have been modelled based on different approaches. Most researchers have considered uniform distribution for the cutting grain over the grinding wheel surface [12,13]. Random and stochastic distribution of the cutting grains has been also considered in literature [14–16].

In this work a coupled empirical model was taken from the work of Hor et al. [17] for the single grain scratch simulation of 100Cr6 steel with cBN grains. DEFORM-3D commercial code was selected for the handling of the single-grain scratch simulation, whose performance was investigated and validated in comparison with the counterpart FEM software [18]. The

Peer-review under responsibility of the International Scientific Committee of 7th HPC 2016 in the person of the Conference Chair Prof. Matthias Putz
doi:10.1016/j.procir.2016.03.179

single-grain scratch characteristics regarding the force values and the chipping mechanism are extended to the aggregate action of cutting grains in grinding process. The extension is performed through defining a suitable probability density function for the random distribution of cutting grains according to the measured topography of the grinding wheel surface by using confocal microscopy. The parameters of the considered Gamma probability density function are accordingly extracted.

2. Modeling of cylindrical grinding process

2.1. FEM simulation of single-grain scratch

The action of a single cBN grain on a 100Cr6 steel workpiece is simulated for two nominal grain sizes (d=76µm and 151µm) and under different cutting conditions (depth of cut and cutting velocity). The grain geometry is considered as lofted hexagonal volumes embedded in spheres with diameters equal to the nominal grain size (Figure 1). Five cutting velocity levels (v_c=10; 20; 30; 40; 50 m/s) and two grain depth of cut levels (a_g=3; 5 µm) are chosen for the FEM simulation. The material properties and the coefficients of the coupled constitutive relation are taken from the work of Hor et al [17]. The normal and tangential force components along with the material removal/ploughing behavior are extracted from the FEM results.

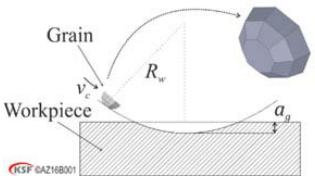

Figure 1. Single-grain scratch kinematics and the grain geometry

In order to quantify the chip formation and material removal characteristics a parameter is defined as the relative chip area η_c. The relative chip area is the ratio of the removed material cross section area $A_c - A_p$ to the ploughed material (pileup) cross section area A_p, and can be expressed as:

$$\eta_c = \frac{A_c - A_p}{A_c} = 1 - \frac{A_p}{A_c} \quad (1)$$

Figure 2 illustrates the geometrical parameters of a single grain scratch and the two areas A_p (dark-hatched) and A_c (light hatched) in the plane normal to the cutting direction. It is assumed that the pileup geometry can be defined by two parameters: pileup height h_p, and pileup angle β. In other words, the pileup volume is equally distributed on the both sides of the scratch, which forms equilateral triangles in the planes normal to the cutting direction.

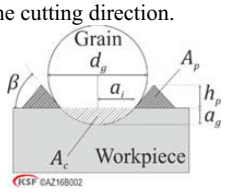

Figure 2. Single grain scratch cross-section areas and parameters

Larger values of relative chip area approaching 1 are favorable in terms of grinding efficiency. A view of the scratch simulated with v_c =20 m/s and d =151 µm grain size with maximum penetration depth of a_g=5 µm normal to the cutting direction and the effective stress distribution are presented in Figure 3. Figure 4 shows the corresponding force components.

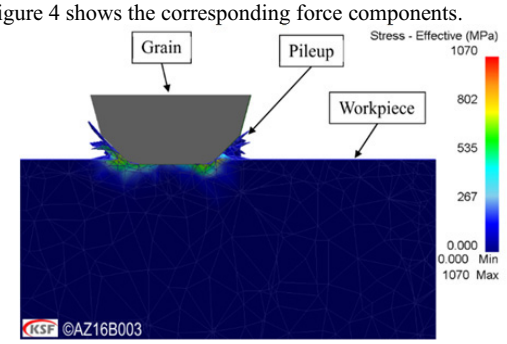

Figure 3. Scratch cross section and the effective stress distribution

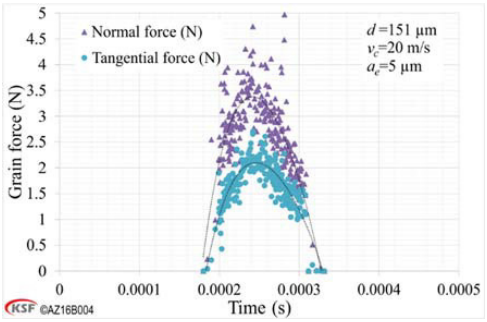

Figure 4. Simulated Normal and tangential force components of a scratch

The variations of the force components and the relative chip area with cutting velocity reflect the dependency of the material properties on the strain-rate. The tangential grinding force and relative chip area values are presented in Figure 5 and Figure 6 respectively.

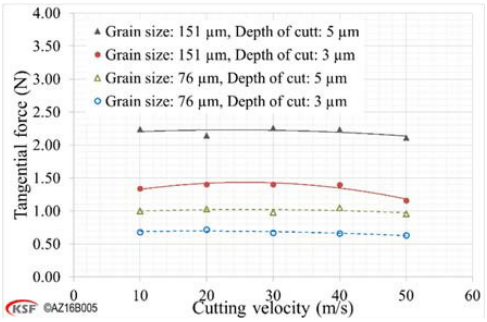

Figure 5. Variations of tangential force with cutting velocity and depth of cut

The increasing and decreasing behavior of the relative chip area with cutting velocity, which is also observed in the force diagram to a smaller degree, can be associated with the coupled material model. In small strain-rate values the work-hardening is the dominant phenomenon, where the chip removal is more

effective and the force components increase. On the other hand, in larger strain-rate values corresponding to higher cutting velocities the thermal softening becomes more dominant. As the result, the force values reduce, the material behavior becomes more ductile and the chip removal becomes less efficient (smaller relative chip area). Figure 6 also shows that sharper grains (smaller grain size) perform material removal more efficiently (larger relative chip area).

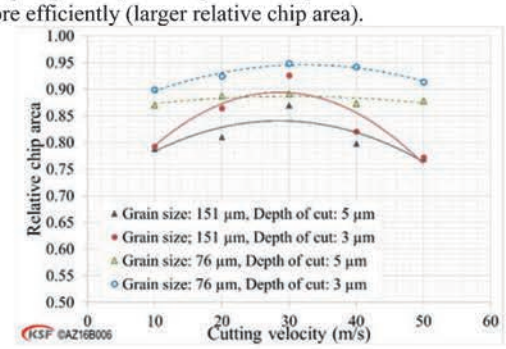

Figure 6. Variations of the relative chip area with cutting velocity and depth

As in the actual grinding process an unlimited grain depth of cut values are encountered, the simulation results for two depth of cut values are regressively extended to the depth of cut of each grain which is determined by the process kinematics.

2.2. Grinding wheel stochastic model

The distribution of cutting grains on the grinding wheel surface is modeled according to the Gamma probability density function for the position of the grains. The shape parameter α_g and the scale parameter λ_g of the Gamma distribution are defined according to the actual topography of a cBN grinding wheel extracted from its confocal microscopy. Figure 7 shows the actual topography of a metal-bonded cBN grinding wheel (B151-C75-MB with 100 mm diameter produced by Baerhausen) and the height distribution along with its Abbott curve.

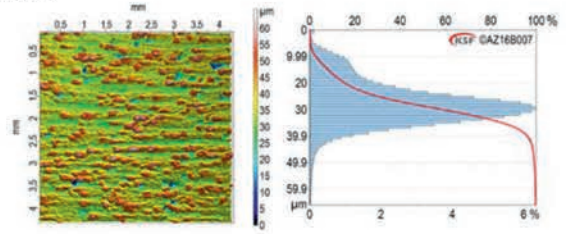

Figure 7. Topography (left), and the histogram and Abbott curve (right) of the metal-bonded cBN grinding wheel

The parameters of the following density function of the grain height (x) are accordingly defined as $\alpha_g = 1.875$ and $\lambda_g = 0.0625$.

$$f_\Gamma(x) = \begin{cases} \frac{\lambda_g{}^{\alpha_g} x^{(\alpha_g-1)} e^{-\lambda_g x}}{\Gamma(\alpha_g)} & x \geq 0 \\ 0 & x < 0 \end{cases} \quad (2)$$

where Γ is the Gamma function. By defining the height of the wheel topography points as radius from the wheel center, the virtual wheel surface model can be generated as shown in Figure 8. The cutting grains are considered as spheres in the virtual wheel model.

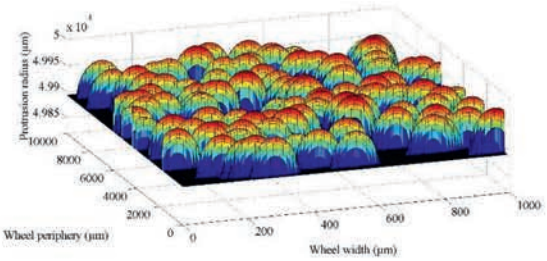

Figure 8. Virtual grinding wheel model based on stochastic grain distribution

2.3. Kinematics of cylindrical grinding

The simulated single-grain scratch can be extended to the aggregate cutting action of abrasive grains on a grinding wheel surface through defining the stochastic distribution of the grains (section 2.2) and the grain-workpiece interaction through the kinematics of the process (equivalent to the kinematics presented in [19] for conventional cylindrical plunge grinding). By expressing the coordinates of the cutting grains (X_i,Y_i) and the individual points on the workpiece surface (X_j,Y_j) in a global coordinate system attached to the workpiece, the grain-workpiece engagement can be characterized and interpreted according to the FEM results. The engagement criteria of the i^{th} grain can be consequently expressed as:

$$(X_i - X_j)^2 + (Y_i - Y_j)^2 + (Z_i - Z_j)^2 < \left({}^{d_i}/_2\right)^2 \quad (3)$$

In the case of engagement (when equation 3 holds), the grinding force components and the workpiece surface topography are calculated according to the engagement depth, grain size and cutting velocity. The generated topography is mainly influenced by the removed and pileup material volumes. The proposed procedure is applied to the whole grains in the wheel-workpiece contact zone at each time step.

3. Results and verification

In order to verify the simulation procedure, cylindrical plunge grinding of 100Cr6 (56 HRC) round bars is performed on an EMAG SN204 CNC cylindrical grinder with oil as grinding fluid. Grinding conditions are presented in Table 1.

Table 1. Cylindrical grinding parameters.

Parameter	Value
Cutting velocity v_c, (m/s)	30; 50
Infeed velocity v_f , (mm/min)	1; 2; 3; 4
Speed ratio $q_s = v_c/v_w$ (-)	60

In the above table v_w is the workpiece velocity which is related to the cutting velocity through the grinding speed ratio q_s. The experimental and simulated normal grinding forces are compared in Figure 9. Although the experimental and simulation results follow the same incremental trend, the simulated forces are considerably larger than the experiments.

This variation could be due to the fact that in real grinding conditions the number of cutting edges gets normally smaller owing to the grain breakage and pull-out which leads to fewer active grains and consequently smaller force values. In addition to that, the actual grains are normally sharper than pure spheres owing to the presence of numerous cutting edges and corners.

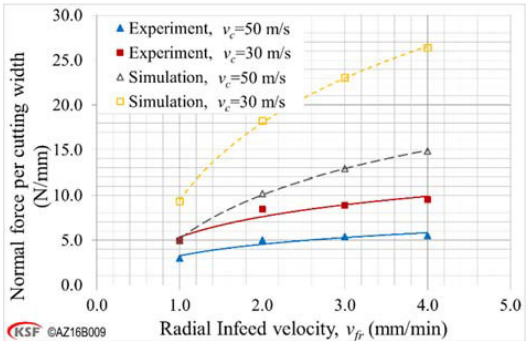

Figure 9. Experimental and simulated normal grinding force values

The simulated ground workpiece topography is presented in Figure 10. The simulated average roughness R_a is about 1.79 µm which is slightly larger than the measured value of 0.89 µm. In addition to the lack of grain breakage in the simulation, this deviation in roughness values can be associated with neglecting the rubbing effect of the bond, which smoothens the workpiece surface.

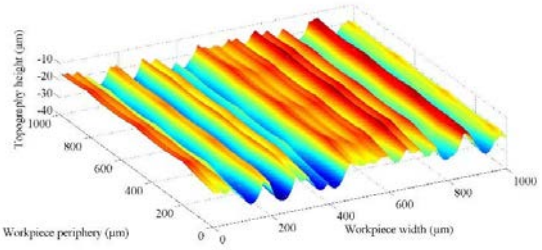

Figure 10. Ground workpiece simulated with v_c=30 m/s and v_f=2 mm/min

4. Conclusion

In this study a coupled (temperature and strain-rate) constitutive material model was used in the FE simulation of a single grain scratch on steel. The model predicts work-hardening and thermal softening domains for the cutting process. It was shown that with the same depth of cut, sharper grains exhibit smaller forces and more efficient material removal.

A virtual grinding wheel model was generated based on the actual wheel topography measurement (confocal microscopy), and a probability density function for the stochastic distribution of the cBN grains. Extension of the FEM force components and material removal performance (chip formation vs. material pileup) to the aggregate action of grains via the grinding kinematics led to the prediction of grinding forces and workpiece surface topography. The simulated force results are qualitatively in accordance with the experiments but their values are larger as the actual grains incorporate extremely sharp edges (smaller forces) in comparison with defined shape assumptions for the cutting grains.

References

[1] D.A. Doman, A. Warkentin, R. Bauer, Finite element modeling approaches in grinding, International Journal of Machine Tools and Manufacture 49 (2009) 109–116.
[2] E. Brinksmeier, J.C. Aurich, E. Govekar, C. Heinzel, H.-W. Hoffmeister, F. Klocke, J. Peters, R. Rentsch, D.J. Stephenson, E. Uhlmann, K. Weinert, M. Wittmann, Advances in Modeling and Simulation of Grinding Processes, CIRP Annals - Manufacturing Technology 55 (2006) 667–696.
[3] F. Klocke (Ed.), Modelling and simulation in grinding, 2003.
[4] A. Ram, J. Danckert, T. Faurholdt, Finite element analysis of stresses due to normal and sliding contact conditions on an elastic surface (2003) 21–34.
[5] Y. Yao, M. Schlesinger, Drake, G. W. F., A multiscale finite-element method for solving rough-surface elastic-contact problems, Canadian Journal of Physics 82 (2004) 679–699.
[6] D.A. Doman, Rubbing and plowing phases in single grain grinding. Dissertation, Halifax, Nova Scotia, Canada, 2006.
[7] F. Klocke, T. Beck, S. Hoppe, T. Krieg, N. Müller, T. Nöthe, H.-W. Raedt, K. Sweeney, Examples of FEM application in manufacturing technology, Journal of Materials Processing Technology 120 (2002) 450–457.
[8] Y. Ohbuchi, T. Obikawa, Finite element modeling of chip formation in the domain of negative rake angle cutting, Journal of Engineering Materials and Technology 125 (2003) 324–332.
[9] A. Shrot, M. Bäker, Determination of Johnson–Cook parameters from machining simulations, Proceedings of the 20th International Workshop on Computational Mechanics of Materials - IWCMM 20 52 (2012) 298–304.
[10] A. Hor, F. Morel, J.-L. Lebrun, G. Germain, Modelling, identification and application of phenomenological constitutive laws over a large strain rate and temperature range, Mechanics of Materials 64 (2013) 91–110.
[11] M. Calamaza, D. Couparda, F. Girotab, Numerical simulation of titanium alloy dry machining with a strain softening constitutive law, Machining Science and Technology 14 (2010) 244–257.
[12] X. Chen, W. Rowe, Analysis and simulation of the grinding process. Part I: Generation of the grinding wheel surface, International Journal of Machine Tools and Manufacture 36 (1996) 871–882.
[13] P. Stępień, Grinding forces in regular surface texture generation, International Journal of Machine Tools and Manufacture 47 (2007) 2098–2110.
[14] H.-C. Chang, Wang, J. -J. Junz, A stochastic grinding force model considering random grit distribution, International Journal of Machine Tools and Manufacture 48 (2008) 1335–1344.
[15] S. Agarwal, P. Venkateswara Rao, Modeling and prediction of surface roughness in ceramic grinding, International Journal of Machine Tools and Manufacture 50 (2010) 1065–1076.
[16] F.W. Pinto, G.E. Vargas, K. Wegener, Simulation for optimizing grain pattern on Engineered Grinding Tools, CIRP Annals - Manufacturing Technology 57 (2008) 353–356.
[17] A. Hor, F. Morel, J.-L. Lebrun, G. Germain, An experimental investigation of the behaviour of steels over large temperature and strain rate ranges, International Journal of Mechanical Sciences 67 (2013) 108–122.
[18] T. Ozel, I. Llanos, J. Soriano, P.-J. Arrazola, 3D Finite Element Modeling of Chip Formation Process for Machining Inconel 718: Comparison of FE Software Predictions, Machining Science and Technology 15 (2011) 21–46.
[19] A. Zahedi, T. Tawakoli, J. Akbari, Energy aspects and workpiece surface characteristics in ultrasonic-assisted cylindrical grinding of alumina–zirconia ceramics, International Journal of Machine Tools and Manufacture 90 (2015) 16–28.